

# Accurate and Efficient Quantum Computations of Molecular Properties Using Daubechies Wavelet Molecular Orbitals: A Benchmark Study against Experimental Data

Cheng-Lin Hong,<sup>1,\*</sup> Ting Tsai,<sup>1,\*</sup> Jyh-Pin Chou,<sup>2,3,\*</sup> Peng-Jen Chen,<sup>2,4</sup> Pei-Kai Tsai,<sup>1</sup> Yu-Cheng Chen,<sup>2</sup> En-Jui Kuo,<sup>1,5</sup> David Srolovitz,<sup>4,6</sup> Alice Hu,<sup>2,7</sup> Yuan-Chung Cheng,<sup>8,9,10</sup> and Hsi-Sheng Goan<sup>1,9,10,†</sup>

<sup>1</sup>*Department of Physics and Center for Theoretical Physics,  
National Taiwan University, Taipei 10617, Taiwan*

<sup>2</sup>*Department of Mechanical Engineering, City University of Hong Kong, Kowloon, Hong Kong SAR 999077, China*

<sup>3</sup>*Department of Physics, National Changhua University of Education, Changhua 50007, Taiwan*

<sup>4</sup>*Hong Kong Institute for Advanced Study, City University of Hong Kong, Kowloon, Hong Kong SAR 999077, China*

<sup>5</sup>*Department of Physics and Joint Quantum Institute,  
University of Maryland, College Park, MD 20742 USA*

<sup>6</sup>*Department of Mechanical Engineering, The University of Hong Kong, Pokfulam, Hong Kong SAR 999077, China*

<sup>7</sup>*Department of Materials Science and Engineering,  
City University of Hong Kong, Kowloon, Hong Kong SAR 999077, China*

<sup>8</sup>*Department of Chemistry, National Taiwan University, Taipei 10617, Taiwan*

<sup>9</sup>*Center for Quantum Science and Engineering, National Taiwan University, Taipei 10617, Taiwan*

<sup>10</sup>*Physics Division, National Center for Theoretical Sciences, Taipei, 10617, Taiwan*

(Dated: May 31, 2022)

Although quantum computation is regarded as a promising numerical method for computational quantum chemistry, current applications of quantum-chemistry calculations on quantum computers are limited to small molecules. This limitation can be ascribed to technical problems in building and manipulating more quantum bits (qubits) and the associated complicated operations of quantum gates in a quantum circuit when the size of the molecular system becomes large. As a result, reducing the number of required qubits is necessary to make quantum computation practical. Currently, the minimal STO-3G basis set is commonly used in benchmark studies because it requires the minimum number of spin orbitals. Nonetheless, the accuracy of using STO-3G is generally low and thus can not provide useful predictions. Herein, we propose to adopt Daubechies wavelet functions as an accurate and efficient method for quantum computations of molecular electronic properties. We demonstrate that a minimal basis set constructed from Daubechies wavelet basis can yield accurate results through a better description of the molecular Hamiltonian, while keeping the number of spin orbitals minimal. With the improved Hamiltonian through Daubechies wavelets, we calculate vibrational frequencies for H<sub>2</sub> and LiH using quantum-computing algorithm to show that the results are in excellent agreement with experimental data. As a result, we achieve quantum calculations in which accuracy is comparable with that of the full configuration interaction calculation using the cc-pVDZ basis set, whereas the computational cost is the same as that of a STO-3G calculation. Thus, our work provides a more efficient and accurate representation of the molecular Hamiltonian for efficient quantum computations of molecular systems, and for the first time demonstrates that predictions in agreement with experimental measurements are possible to be achieved with quantum resources available in near-term quantum computers.

## I. INTRODUCTION

Quantum computation has recently emerged as a revolutionary numerical scheme for computational quantum chemistry [1–4], which plays crucial roles in the design of novel materials and drugs. Quantum simulation has been successfully applied to the determination of the structural and electronic properties of small molecules [5–12], and is considered as the most promising near-term and real-world applications of quantum computation. Specifically, quantum algorithms for solutions of molecular energies have the unique ability to provide exact results

even for chemical systems with high computational complexity. On classical computers, the complexity of exact quantum chemical computations scales exponentially with system size. As a result, classical approaches such as the full configuration interaction (FCI) method are restricted to small molecules, and approximations, such as truncated configuration interactions or the coupled-cluster (CC) approach, are required to reduce the computational complexity to make them tractable on classical computers. Even so, such accurate quantum-chemistry methods are still not practical for molecules of medium or large size. Such problems of high classical complexity represent a sweet spot for quantum computing in quantum chemistry to demonstrate quantum advantage.

The advantage of applying quantum-computing algorithms to computational quantum chemistry hangs on a significant reduction in the computational complexity;

\* Contributed equally to this work.

† goan@phys.ntu.edu.tw

the computational complexity of quantum-computing algorithms for quantum chemistry grows in a polynomial manner with increasing system size, and thus classically intractable computations become tractable on quantum computers [1]. At the moment, the number of quantum bits (qubits) and the length (depth) of the quantum circuits that can be reliably performed in current noisy intermediate-scale quantum (NISQ) devices [13] have limited the size of molecules that can be calculated. As the power, quality and capability of quantum computers have improved significantly in the last few years and will continue to advance rapidly, one can expect that the quantum-computing algorithms will become a powerful tool for computational quantum chemistry. Nevertheless, innovative methods that can reduce the quantum resources required for quantum simulations of molecular systems are crucial in order to provide solutions to large molecules.

Among the quantum algorithms for molecular properties, the quantum phase estimation (QPE) algorithm [14–17] and the variational quantum eigensolver (VQE) algorithm [8, 18–21] are currently the two most promising methods for solving electronic structure problem in quantum-computational chemistry. Researches in recently years have shown that implementing the QPE algorithm typically requires a large number of quantum operations, and hence it may require a future quantum computer with quantum error correction to solve chemical problems for large molecules. Therefore, in this work we focus on the VQE method, a hybrid quantum-classical algorithm, for near-term NISQ hardware. The process of performing a quantum computation on chemical systems using the VQE method can be described in the following steps: (1) Perform a computation on a classical computer using traditional quantum-chemistry methods to prepare the reference Hartree-Fock (HF) state. (2) Construct a many-body Hamiltonian in the second quantization form based upon single-particle solutions obtained from the previous step. (3) Choose an *ansatz*, such as the chemically inspired *ansatz* of the unitary coupled-cluster with single and double excitations (UCCSD) or the heuristic hardware-efficient *ansatz* with parameterized gates, to express the many-body wave function, resulting in a designed quantum circuit with adjustable variational parameters. (4) Perform the calculation and then the measurement of the parameterized quantum circuit to solve for the eigenvalues of the given many-body problem, i.e., the total energy of the system by summing the expectation value of each term in the Hamiltonian estimated through repeated state preparation and measurement. (5) Perform an energy minimization to search for the lowest eigenvalue by tuning the adjustable parameters, which is carried out on a classical computer. Updated parameters are passed into the quantum circuit to iteratively refine the wave function until the minimization of the energy is achieved.

In addition to the quantum algorithm, the choice of basis set is also of prime importance in quantum chemistry

on quantum computers. Quantum simulation of molecular systems could be realized in either a first quantized or second quantized form. The former one represents the molecular Hamiltonian on a multidimensional grid of many-electron coordinates, and hence requires a large number of qubits to carry out the quantum computation, which is still unavailable on today’s quantum computers. Therefore, realizable quantum algorithms for quantum chemistry depend on the second quantized form of the molecular Hamiltonian, which is parameterized using molecular orbitals and parameters calculated from a classical HF calculation. As a result, the choice of the basis set determines the quality of the constructed Hamiltonian. Although minimal basis sets, such as the STO-3G basis [22], has proven to be extremely valuable for developing and benchmarking new quantum-computational algorithms [3, 8, 23], the accuracy that can be obtained using minimal basis sets tends to be poor when compared with the experimental data due to the incompleteness of the chosen orbitals. In order to most efficiently utilize quantum resources, which are scarce in available quantum computers, it is of critical importance to minimize the number of orbitals required while preserving the quality of the second quantized Hamiltonian.

Currently, basis sets constructed from Slater-type orbitals (STOs) are widely used in classical computational chemistry (largely for their simplicity). To improve accuracy, high-level basis sets, such as 6-31G [24] and cc-pVDZ [25] basis sets, are regularly employed in computational chemistry, but at the cost of increased computational loading. Due to the limited size and available circuit depth in nowadays quantum computers, quantum computations using high-level basis sets remain intractable. Consequently, identifying a suitable basis set is essential for accurate *and* efficient quantum computation. In this regard, various methods utilizing truncated molecular orbital space (active space) to reduce required quantum resources have been proposed. More specifically, a reduction in the active space based on selected natural molecular orbitals has been proposed and applied to quantum-chemistry calculations on quantum computers with a certain degree of success [3]. It is also possible to increase the accuracy of truncated active-space calculations with classical postprocessing [26]. Nevertheless, these methods rely on additional classical post-HF calculations that could become intractable quickly for medium-size molecules. Notably, in a series of recent papers, Aspuru-Guzik and coworkers presented an efficient approach to simulate molecular systems by using a combination of multiresolution analysis of molecular wave functions and pair-natural orbitals on the level of second-order perturbation theory [27, 28]. Their work demonstrates that the qubit requirements can be significantly reduced by adopting a preoptimized basis-set-free representation of the molecular Hamiltonian based on wavelet-based numerical techniques. However, although a systematic procedure to determine a high-quality Hamiltonian is proposed in these papers, the multiresolution

analysis (MRA) approach is treated as a black box, and the extent of benefits gained by using the preoptimized orbitals has not been fully elucidated.

In this work, we introduce minimal basis sets consisting of Daubechies wavelet functions [29] to achieve high-quality small-size basis sets for quantum simulation of molecular systems [30]. Daubechies wavelet basis sets have been shown to yield accurate results with excellent computational efficiency as compared with contracted Gaussian basis sets for large molecules [31, 32], and we believe that applications of quantum-computing algorithms to computational chemistry could also benefit from the adoption of Daubechies wavelet basis sets. Thus, the main goal of this work is to examine the use of Daubechies wavelet basis sets to improve the accuracy and efficiency of quantum computations of chemical systems: the optimized molecular orbitals constructed from Daubechies wavelet functions should yield a high-quality second-quantized Hamiltonian and improve the accuracy of the VQE calculations. Moreover, it is important to critically compare quantum-computation results with experimental values in order to evaluate the true potential of quantum-computational methods for quantum chemistry. Therefore, we choose to benchmark calculated vibration frequencies for H<sub>2</sub> and LiH with experimental values. In the following, we present a prescription to construct Daubechies wavelet basis for high-quality second-quantized Hamiltonians for molecular systems, and show that a minimal basis prepared in this way leads to significantly more accurate results in terms of molecular properties compared to experimental data.

## II. METHODOLOGY

### A. The Daubechies wavelet molecular orbitals

The choice of a basis set plays a critical role in determining the performance of a quantum-chemistry calculation. Atomic orbitals are an intuitive choice of basis set for isolated molecular systems. Nonetheless, basis sets constructed from atomic orbitals suffer from nonorthogonality and hence require additional computations of the overlap matrices. For this reason, orthogonal basis sets constructed from localized orbitals have been proposed and are now in widespread use for quantum-chemistry calculations.

Daubechies wavelets provide an alternative option for basis sets in computational quantum chemistry [31–33]. In wavelet theory, there are two fundamental functions, a scaling function  $\phi(x)$  and a wavelet  $\psi(x)$ :

$$\begin{aligned}\phi(x) &= \sqrt{2} \sum_{j=1-m}^m h_j \phi(2x - j), \\ \psi(x) &= \sqrt{2} \sum_{j=1-m}^m g_j \phi(2x - j),\end{aligned}\tag{1}$$

where the coefficients  $h_j$  and  $g_j = (-1)^j h_{-j+1}$  are elements of the filter characterizing the order  $m$  wavelet family. In this work, we adopt the dual-resolution Daubechies wavelet grids as implemented in the BigDFT code [33–35]. There, the three-dimensional basis functions  $\phi_{i,j,k}(\mathbf{r})$  are a tensor product of the one-dimensional scaling function on the grid  $(i, j, k)$  with uniform mesh  $h'$  for grid points away from the nucleus,

$$\phi_{i,j,k}(\mathbf{r}) = \phi(x/h' - i)\phi(y/h' - j)\phi(z/h' - k),\tag{2}$$

whereas for grid points close to the nucleus, a “fine” region with the same uniform mesh  $h$  can be described with

$$\phi_{i,j,k}(\mathbf{r}) = \phi(x/h - i)\phi(y/h - j)\phi(z/h - k),\tag{3}$$

augmented by a set of seven wavelets ( $\psi_{i,j,k}^v$ ,  $v = 1\dots7$ ),

$$\begin{aligned}\psi_{i,j,k}^1(\mathbf{r}) &= \psi(x/h - i)\phi(y/h - j)\phi(z/h - k), \\ \psi_{i,j,k}^2(\mathbf{r}) &= \phi(x/h - i)\psi(y/h - j)\phi(z/h - k), \\ \psi_{i,j,k}^3(\mathbf{r}) &= \psi(x/h - i)\psi(y/h - j)\phi(z/h - k), \\ \psi_{i,j,k}^4(\mathbf{r}) &= \phi(x/h - i)\phi(y/h - j)\psi(z/h - k), \\ \psi_{i,j,k}^5(\mathbf{r}) &= \psi(x/h - i)\phi(y/h - j)\psi(z/h - k), \\ \psi_{i,j,k}^6(\mathbf{r}) &= \phi(x/h - i)\psi(y/h - j)\psi(z/h - k), \\ \psi_{i,j,k}^7(\mathbf{r}) &= \psi(x/h - i)\psi(y/h - j)\psi(z/h - k).\end{aligned}\tag{4}$$

The basis functions on the fine grid and the coarse grid, which is half as dense as the fine one, can be derived from Eq. (1).

The advantages of Daubechies wavelets are as follows. First, wavelets are localized in both real and reciprocal space. Localization in real space is essential for efficient calculations of isolated systems. Localization in reciprocal space, on the other hand, is important for preconditioning since it provides approximate eigenfunctions of the kinetic energy operator. Therefore, the Daubechies wavelet basis provides an accurate representation of molecular Hamiltonian in spatially localized grid points. In this regard, it is closely related to the recently proposed plane-wave dual-basis approach for low-depth quantum simulation of materials [36, 37]. Second, the completeness of the Daubechies wavelet basis set eliminates the superposition error induced by the incompleteness of basis sets like STO-3G. Third, the use of wavelets as basis sets provides strong adaptivity in programming. In the particular implementation used in this work, the space is simulated using fine and coarse grids. The former is used to describe the region containing the chemical bonds and the latter for the region of exponentially decaying wave-function tails. As a result, the wavelets with a reasonable grid size provide a basis higher in quality than most contracted Gaussian basis sets [29, 31]. These characteristics make chemical accuracy achievable at a more affordable computational cost.

Performing quantum simulation of molecular energy directly on a Daubechies wavelet basis would be intractable due to the large number of grid points. Nevertheless, it has been demonstrated that a self-consistent

field calculation with Daubechies wavelets yields molecular orbitals suitable for quantum-chemistry calculations. Furthermore, a high-quality minimal basis set using low-lying molecular orbitals constructed from Daubechies wavelet yields very accurate results in density-functional calculations [31–34]. Note that in this manner we take advantage of both the accurate representation of the Daubechies wavelet grid method and the reduced size of a minimal basis.

A molecular orbital (MO) can be constructed from Daubechies wavelet functions by superposition of the the integer-translated scaling functions and wavelets centered at the grid points in the computational domain. Therefore, a MO basis function  $\chi(\mathbf{r})$  can be expressed as

$$\chi(\mathbf{r}) = \sum_{i,j,k} S_{i,j,k} \phi_{i,j,k}(\mathbf{r}) + \sum_{i,j,k} \sum_{v=1}^7 D_{i,j,k}^v \psi_{i,j,k}^v(\mathbf{r}), \quad (5)$$

where  $S_{i,j,k}$  and  $D_{i,j,k}$  are the expansion coefficients. In a typical calculation, the coefficients can be optimized iteratively in a HF self-consistent-field (SCF) calculation, producing a large set of optimized MOs each represented by Daubechies wavelets. A minimal number of MOs can then be selected from these HF-SCF MOs to form a minimal basis set. This set of *minimal basis Daubechies wavelet molecular orbitals* is constructed in a much larger Hilbert space spanned by the grid of Daubechies wavelet functions and also adapted to the structure of the molecule in the HF-SCF calculation. Naturally, the Daubechies wavelet minimal basis set thus constructed would have a higher quality compared with conventional minimal basis set such as the STO-3G basis, although with the same number of basis MOs. The number of spin orbitals is one of the main factors that determines the numerical expense of quantum computing. Therefore, accurate quantum computations with fewer spin orbitals (and hence less qubits and lower quantum circuit depth needed) are highly desired for practical computational chemistry. In this work, the Daubechies wavelet molecular orbitals are obtained by performing a HF calculation using the BigDFT code [33, 34], an *ab initio* software package that employs Daubechies wavelet basis sets. From the BigDFT output, we select a minimal number of spin orbitals to form a set of minimal basis Daubechies wavelet molecular orbitals for the following quantum simulations. We refer the interested readers to Ref. [29] for a more detailed discussion of Daubechies wavelets.

## B. Second-quantized Hamiltonian

Given a set of molecular orbitals, one can construct the many-body Hamiltonian in the following second quantization form:

$$H = \sum_{pq} h_{pq} a_p^\dagger a_q + \frac{1}{2} \sum_{pqrs} h_{pqrs} a_p^\dagger a_q^\dagger a_r a_s, \quad (6)$$

where

$$h_{pq} = \int d\mathbf{x} \chi_p^*(\mathbf{x}) \left( -\frac{\nabla^2}{2} - \frac{Z}{|\mathbf{r} - \mathbf{R}|} \right) \chi_q(\mathbf{x}), \quad (7)$$

$$h_{pqrs} = \int d\mathbf{x}_1 d\mathbf{x}_2 \frac{\chi_p^*(\mathbf{x}_1) \chi_q^*(\mathbf{x}_2) \chi_r(\mathbf{x}_2) \chi_s(\mathbf{x}_1)}{|\mathbf{r}_1 - \mathbf{r}_2|}. \quad (8)$$

In this study, we take advantage of the minimal basis Daubechies wavelet molecular orbitals provided by the BigDFT code to construct second-quantized Hamiltonians. In BigDFT, the MO wave function is constructed by real-space wavelets, in which the grid spacing would control the accuracy. We therefore perform convergence tests on different grid parameters to determine the best resolution. Additionally, unlike calculations with the Gaussian-type basis, our calculations treat the core electrons of a given molecule using GTH-HGH pseudopotentials [38, 39]. After selecting suitable grid parameters, with the permutation symmetries of the electron integrals, the one-electron integrals  $h_{pq}$  can be directly calculated via the BigDFT code, and we need to add a Poisson solver [40, 41] to evaluate the two electron integrals  $h_{pqrs}$ .

Moreover, in order to gain insights into the accuracy of the minimal basis Daubechies wavelet method, we also carry out calculations using the STO-3G molecular orbitals. In this case, the coefficients  $h_{pq}$  and  $h_{pqrs}$  are computed from one- and two-electron integrals using the built-in function in PSI4 for STO-3G calculations.

## C. Quantum computation

In order to solve for the electronic energy from the second-quantized Hamiltonian using quantum computation, parity encoding [42, 43] is performed to transform the second-quantized fermionic operators in Eq. (6) to qubit operations in a quantum circuit. The  $\mathbb{Z}_2$  symmetry is exploited to further reduce the number of qubits [44] required to carry out the calculation. Furthermore, we apply the VQE approach to calculate molecular energies. If we parameterize the trial wave function  $|\Psi(\vec{\theta})\rangle$  (*ansatz*), the variational principle guarantees that

$$E(\vec{\theta}) \equiv \langle \Psi(\vec{\theta}) | \mathcal{H} | \Psi(\vec{\theta}) \rangle \geq E_0. \quad (9)$$

where  $E_0$  is the ground-state energy of Hamiltonian  $\mathcal{H}$  evaluated by a quantum circuit. Consequently, we use the classical LBFGS-B optimization method [45] to update parameters and pass into the quantum circuit to iteratively refine the wave function to reach minimal energy.

In order to account for electronic correlations, the many-body wave function is expressed in the unitary coupled-cluster (CC) *ansatz*. We restrict the CC expansion to single and double excitations; i.e., the UCCSD *ansatz* [18, 20, 46, 47] or a low-depth heuristic circuit. To benchmark the performance of the minimal basis

Daubechies wavelet method, we focus on the better-defined UCCSD *ansatz* first. Trotterization [48] is applied to simplify the excitation operators in this *ansatz*. Previous studies suggest that first-order trotterization is adequate for UCCSD calculations [49], and different orderings of the operators in the Trotterized form of UCC methods [50] could be employed. We reorder the excitation operator (descending order from classical MP2 contribution) to construct the UCCSD *ansatz*. Although the UCCSD *ansatz* provides high-quality representation of the trial wave function, the challenge of implementing UCCSD *ansatz* on quantum computer is its steep requirement of circuit depth which scales as  $\mathcal{O}\left(\binom{N_{\text{occ}}}{2} \times \binom{N_{\text{virt}}}{2} \times N_{\text{qubits}}\right)$  [51], where  $N_{\text{occ}}$  ( $N_{\text{virt}}$ ) is the number of occupied (virtual) orbitals that take part in the excitation, where  $\binom{N}{m} = \frac{N \cdot (N-1) \cdots (N-m+1)}{m!}$ . The huge circuit depth means that the UCCSD *ansatz* is not applicable for large molecules in the NISQ era. Hence, we also benchmark the low-depth heuristic *ansatz* to replace the UCCSD *ansatz* on the noisy circuit to reduce the noisy effect. Molecular orbitals obtained by using the Daubechies wavelet and STO-3G basis sets are employed to construct the many-body Hamiltonian, which is solved with the aid of quantum computing, as described above. Calculations with STO-3G molecular orbitals and minimal basis Daubechies wavelet molecular orbitals in the UCCSD *ansatz* are denoted as STO-3G/UCCSD and DW/UCCSD, respectively. All the quantum computations are performed using the IBM Qiskit quantum simulators [52].

### III. RESULTS

#### A. Performance of the minimal basis Daubechies wavelet MOs

We first investigate the optimized molecular structures as well as the vibrational frequencies calculated with quantum computations for small systems including  $\text{H}_2$ , LiH and  $\text{BeH}_2$ . The numbers of spin orbitals included in the calculations using STO-3G (denoted as STO-3G/UCCSD) and minimal basis Daubechies wavelet molecular orbitals (denoted as DW/UCCSD) are 4, 10 and 12 for  $\text{H}_2$ , LiH, and  $\text{BeH}_2$ , respectively, as listed in Table I together with the optimized bond lengths and vibrational frequencies. Note that we choose to focus on the bond length and vibrational frequency because they are measurable molecular properties of which accurate experimental data are available (also listed in Table I). The required number of qubits is generally equal to that of spin orbitals. However, the number of qubits may be reduced by two in parity encoding with  $\mathbb{Z}_2$  reduction. Then the numbers of qubits used for  $\text{H}_2$  and LiH and  $\text{BeH}_2$  in our calculations are 2, 8, and 10, respectively.

In order to evaluate the accuracy achievable using the minimal basis Daubechies wavelet molecular orbitals, we

compare quantum simulation results with classical FCI calculations using traditional 6-31G, cc-pVDZ and cc-pVTZ basis sets, denoted as 6-31G/FCI, cc-pVDZ/FCI and cc-pVTZ/FCI, respectively. For these basis sets, FCI calculations are performed on a classical computer with the Psi4 [53–55] code. With the frozen-core approximation, the numbers of spin orbitals used in 6-31G/FCI are 8, 20, and 24, in cc-pVDZ/FCI are 20, 36 and 46 and in cc-pVTZ/FCI are 56, 86, and 114 for  $\text{H}_2$ , LiH, and  $\text{BeH}_2$ , respectively. Additionally, to clarify whether the truncated Daubechies MO wavelet basis improves accuracy over a conventional basis set with truncation in the MOs, we also consider a cc-pVDZ calculation with truncated unoccupied MOs (denoted as cc-pVDZ\*). The final numbers of orbitals used for each molecule in different basis sets are also listed in Table I.

Due to the simplicity of the  $\text{H}_2$  molecule, all methods give reasonable bond lengths as compared with experimental results. On the other hand, the vibrational frequency shows significant basis set and computational method dependence. Clearly, the STO-3G calculations significantly overestimated the vibrational frequency, while the DW/UCCSD quantum simulation yields results that are comparable in accuracy with the high-level cc-pVTZ/FCI results. The comparison clearly demonstrates the advantage of the Daubechies wavelet molecular orbitals. It also shows that bond length might not be a proper indicator for the quality of computational methods; however molecular properties such as the vibrational frequency provides a more sensitive indicator for the performance of the computational methods.

For LiH and  $\text{BeH}_2$ , however, DW/UCCSD, cc-pVDZ\*/UCCSD, cc-pVDZ/FCI and cc-pVTZ/FCI yield bond lengths that agree well with the experimental values. Notably, those obtained using STO-3G are particularly poor. It is also noted that the accuracy with the assistance of quantum computing (STO-3G/UCCSD) is barely improved, indicating the importance of choosing a proper basis set (and hence an accurate representation of the molecular Hamiltonian). Quantum computing cannot make up the deficiency inherited from a low-quality basis set. Note that the number of spin orbitals used in DW/UCCSD calculations is significantly less than that used in the cc-pVDZ/FCI and cc-pVTZ/FCI calculations. That means optimized molecular orbitals in the Daubechies wavelet are very effective in achieving accurate results with significantly reduced computational resources, making it favorable for quantum simulations.

The potential energy curves (bond dissociation curves) and corresponding errors for molecules  $\text{H}_2$ , LiH and  $\text{BeH}_2$  are shown in Fig. 1. Representations of Hamiltonians using different basis sets for calculations are abbreviated with *basis-name*( $N_e, N_{\text{orb}}$ ), where  $N_e$  and  $N_{\text{orb}}$  represent the number of electrons and spin orbitals, respectively. The error is defined as the absolute energy difference with respect to the ground-state energy value from the exact diagonalization (FCI) in the largest affordable Gaussian basis set of cc-pVTZ considered here. Since STO-

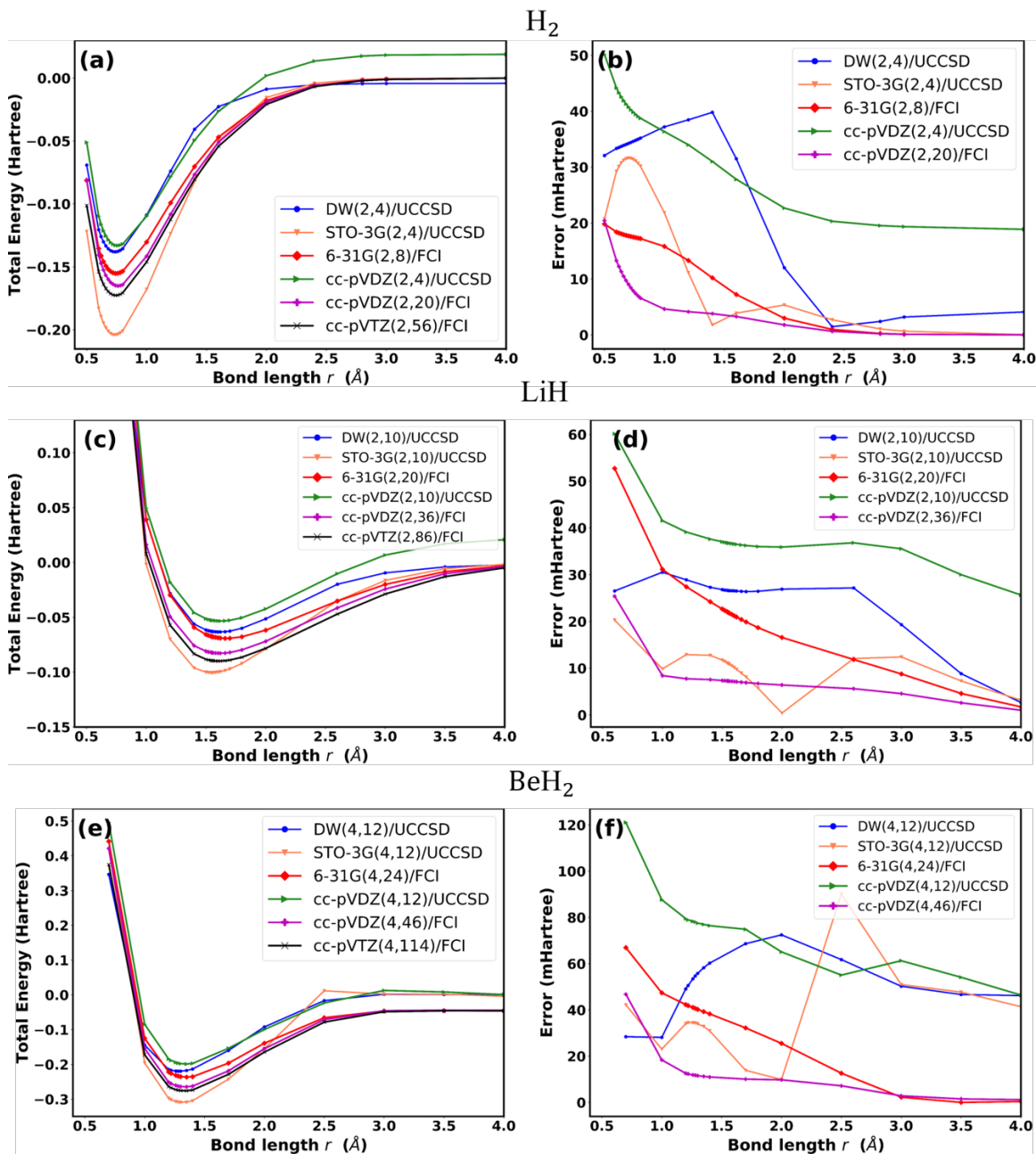


Figure 1. Potential energy curves in (a), (c), and (e) and corresponding errors in (b), (d) and (f) for  $H_2$ ,  $LiH$  and  $BeH_2$ , respectively. The potential energies are computed with VQE on a quantum computer simulator or by exact diagonalization (FCI) on a classical computer. All curves are denoted with  $basis(N_e, N_{orb})/method$ , where  $N_e$  and  $N_{orb}$  represent the numbers of electrons and spin orbitals, respectively. The error is defined as the absolute energy difference with respect to the ground-state energy value from the exact diagonalization (FCI) in the largest affordable Gaussian basis set of cc-pVTZ (in black curve) considered here. The position of the minimum energy and the curvature near the minimum of the potential energy curve give the equilibrium bond length and vibrational frequency of the molecule, respectively. Note that we use the same number of spin orbitals as the STO-3G minimal basis set for the minimal DW basis and the cc-pVTZ\* basis with unoccupied orbitals frozen.

3G/FCI and STO-3G/UCCSD do not exhibit significant differences, only the latter is shown and discussed. Inspection of Fig. 1 reveals that the curvature around the optimized bond length seems to depend strongly on the methods used, implying that the presented vibrational frequency may be a good indicator to benchmark the

performance of the methods. Indeed, the accuracy of the calculated vibrational frequency strongly depends on the basis set used (see Table I). STO-3G tends to overestimate the vibrational frequency by  $> 10\%$ . The accuracy is better in the 6-31G/FCI calculations, albeit at higher computational cost. Both the  $H_2$  and  $LiH$

Table I. Structural property calculations for H<sub>2</sub>, LiH and BeH<sub>2</sub> using different basis sets. The result from a given basis set is denoted with the abbreviation *basis/method*, e.g., the minimal Daubechies wavelet basis calculated by the method of quantum-computing UCCSD ansatz is represented by DW/UCCSD. The total number of spin orbitals used in the calculation is denoted as  $n_{\text{orb}}$ . The equilibrium bond lengths are obtained from the minimum energy positions and the vibrational frequencies are obtained from the curvatures near the optimized (minimum-energy) bond lengths of the potential energy curves in Figs. 1 (a), (c), and (e), respectively.

Basis set	H <sub>2</sub>				LiH				BeH <sub>2</sub>		
	$n_{\text{orb}}$	$R_{\text{H-H}}$ (Å)	$\omega$ (cm <sup>-1</sup> )	$\omega$ error (%)	$n_{\text{orb}}$	$R_{\text{H-Li}}$ (Å)	$\omega$ (cm <sup>-1</sup> )	$\omega$ error (%)	$n_{\text{orb}}$	$R_{\text{H-Be}}$ (Å)	$\omega$ (cm <sup>-1</sup> )
STO-3G/UCCSD <sup>a</sup> .	4	0.74	4930.0	12.0	10	1.55	1674.3	19.1	12	1.32	2273,52
DW/UCCSD	4	0.74	4468.7	1.53	10	1.61	1367.1	2.73	12	1.29	1948.43
6-31G/FCI <sup>b</sup>	8	0.75	4371.6	0.67	20	1.67	1281.7	8.81	24	1.35	1959.1
cc-pVDZ* <sup>c</sup> /UCCSD	4	0.76	4315.2	1.95	10	1.62	1372.2	2.38	12	1.34	$\Delta$ <sup>d</sup>
cc-pVDZ/FCI	20	0.76	4382.7	0.42	36	1.62	1369.5	2.56	46	1.34	2032.1
cc-pVTZ/FCI	56	0.74	4411.0	0.22	86	1.61	1391.9	0.97	114	1.33	2029.7
Experiment [56]	...	0.74	4401.2	...	...	1.60	1405.5	...	...	1.32	X <sup>e</sup>

<sup>a</sup> UCCSD: Quantum computing UCCSD ansatz method performed on a quantum simulator

<sup>b</sup> FCI: Classical exact diagonalization method.

<sup>c</sup> Restricted active space: the number of spin orbitals used is the same as that of the STO-3G minimal basis set.

<sup>d</sup> Nonsmooth potential energy curve in the region near the optimized (minimum-energy) bond length .

<sup>e</sup> No experimental data for the vibrational frequency of the symmetric stretch mode of BeH<sub>2</sub>.

Table II. Nonparallelity errors (NPEs) in unit of mHartree for different basis sets. NPE is defined as the absolute difference between the maximum and minimal errors with respect to a reference on a given potential energy curve. The used reference here is the largest affordable Gaussian basis set of cc-pVTZ shown in Fig. 1.

Basis	H <sub>2</sub>	LiH	BeH <sub>2</sub>
STO-3G/UCCSD	31.58	19.88	80.25
DW/UCCSD	38.33	27.86	44.32
6-31G/FCI	19.84	51.06	66.91
cc-pVDZ* <sup>a</sup> /UCCSD	31.29	34.47	74.60

<sup>a</sup> Restricted active space: the number of spin orbitals used is the same as that of the STO-3G minimal basis set.

vibrational frequencies calculated using cc-pVDZ/FCI, cc-pVTZ/FCI and DW/UCCSD are in excellent agreement with the experimental values. We can also see from Table I that the vibrational frequency of the symmetric stretch mode for BeH<sub>2</sub> calculated using DW/UCCSD is also in agreement with that obtained from the large basis sets of cc-pVDZ/FCI and cc-pVTZ/FCI. Nevertheless, the later two large basis calculations require a large number of MOs, and cannot be realized on near-term quantum devices. Note that although the calculations of cc-pVDZ\*/UCCSD with a restricted active space also generate pretty good results in bond length and vibrational frequency for H<sub>2</sub> and LiH, their potential energy curve errors shown in Figs. 1(b), 1(d), and 1(f) are generally larger than those of DW/UCCSD; besides, the potential energy curve near the optimized equilibrium bond length of BeH<sub>2</sub> generated by cc-pVDZ\*(4,12)/UCCSD is not smooth to allow a calculation of the vibrational frequency, and such an issue might be originated from a convergence issue caused by the truncation in the active space. Similarly, in Ref. [27], Kottmann *et al.* showed

that a MRA(4,12)/UpCCGSD approach that uses the same electron number and spin-orbital number as the minimal basis set does not always converge toward the best solution, and thus fails to produce a smooth potential energy curve for the BeH<sub>2</sub> molecule. In contrast, the minimal basis DW(4,12)/UCCSD method consistently produces a smooth potential energy curve for the BeH<sub>2</sub> molecule. In addition, nonparallelity error (NPE), defined as the absolute difference between the maximum and minimal errors with respect to a reference on a given potential energy surface [27, 57], could be another accuracy metric to describe the full potential energy curve properties. One can see from Table II that DW/UCCSD provides smaller values of NPE for the more complex molecules of LiH and BeH<sub>2</sub>. These results, again, depict the merits of the minimal basis Daubechies wavelet molecular orbitals in calculation of molecular properties.

## B. Molecular structure of water

To further investigate the accuracy of the DW/UCCSD quantum simulation method, we apply it to compute the bond length and bond angle of the optimized geometry of the water molecule and compare the results with those obtained from classical methods. This is a larger molecule with a nonlinear geometry, therefore it represents a more stringent test for the computational methods. The computational results are listed in Table III. In addition, for H<sub>2</sub>O, a potential energy surface (PES) swept over a range of bond lengths and angles is displayed in Fig. 2. Again, the STO-3G calculations yield poor results compared to the experimental data. In contrast, the use of minimal basis Daubechies wavelet molecular orbitals provides significant improvements in the predicted bond length and bond angle when compared with the ex-

Table III. Structural property calculations of water molecule using different basis sets. The result from a given basis set is denoted with the abbreviation *basis/method*. The total number of spin orbitals used in the calculation is denoted as  $n_{\text{orb}}$ . The equilibrium bond length and bond angle are obtained from the minimum-energy position coordinate of the corresponding two-dimensional potential energy surface.

Basis set	H <sub>2</sub> O		
	$n_{\text{orb}}$	$R_{\text{O-H}}$ (Å)	H-O-H angle (°)
STO-3G/FCI	12	1.03	96.7
STO-3G/UCCSD	12	1.03	96.9
DW/UCCSD	12	0.94	106.0
6-31G/FCI	24	0.98	109.0
cc-pVDZ(8,12)/UCCSD	12	0.96	104.0
cc-pVDZ(8,46)/FCI	46	0.97	101.9
Experiment [56]	...	0.96	104.5

perimental values, with a prediction in bond angle even better than the cc-pVDZ/FCI method. Note that the number of spin orbitals used in DW/UCCSD for water is only 12, compared to 48 used in cc-pVDZ/FCI. Clearly, the Daubechies wavelet method significantly improves both the accuracy and efficiency for quantum computations. Note that cc-pVDZ(8,12)/UCCSD in a restricted active space yields a better result in bond length and bond angle than its full CI counterpart [cc-pVDZ(8,46)/FCI], indicating the existence of a possible error cancellation that leads to the good agreement in the restricted active-space case. In other words, the truncated cc-pVDZ(8,12)/UCCSD method yields an improved result in the H<sub>2</sub>O case due to accidental error cancellation, which cannot be expected to be applicable to general molecular systems. In a typical atomic basis set, the calculation result is sensitive to the active-space selection, and how to select an appropriate active space for calculations is highly nontrivial. The poor performance of the STO-3G basis is expected, since the basis lacks the polarization functions with higher orbital angular momentum that are required to accommodate a more flexible angular orientations in bonding. On the other hand, the Daubechies wavelet molecular orbitals constructed from large real-space grids of the wavelet functions can better capture orbital angular dependence properties, yielding a better Hartree-Fock wave function for consistent results, and hence provide the ability to better adapt to flexible molecular structures.

Our results demonstrate that calculations of ground-state molecular properties using minimal basis Daubechies wavelet molecular orbitals can be as accurate as those using cc-pVDZ, but with much fewer spin orbitals. This is especially important for quantum simulations. For the classical segment of the calculation, it determines the computational loading of the two-electron integral, which is the most time-consuming part. For the quantum part, on the other hand, the required number of qubits and the depth of the quantum circuit depend on the number of spin orbitals, and

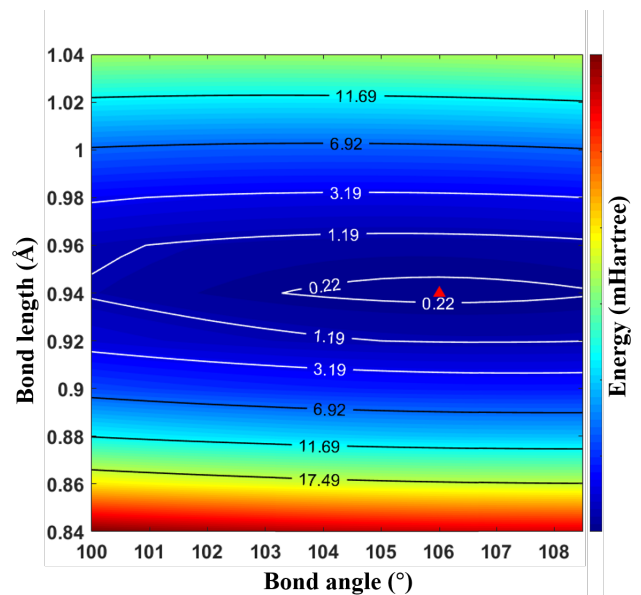


Figure 2. Two-dimensional DW/UCCSD potential energy surface of H<sub>2</sub>O. Color representation of the energy is depicted by the color bar on the right and the energy of the optimized structure, marked by the red triangle, is set to zero.

the available quantum resources are extremely limited, thus providing a strong motivation to reduce the basis size. Quantum computing with the STO-3G basis set can perform due to the small basis set size but its accuracy is generally low and thus can not provide useful predictions. The 6-31G basis set as well as even larger ones require many spin orbitals, and thus quantum computing with these basis sets at the current stage may be impractical. We show that the Daubechies wavelet approach is a highly accurate and efficient alternative for the preparation of the HF reference state that could enable quantum-computing algorithms for larger systems.

### C. Daubechies wavelet Hamiltonian and the effect of noise

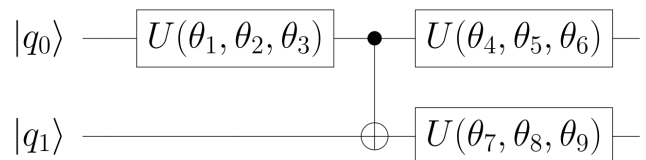


Figure 3. Two-qubit heuristic circuit ansatz for H<sub>2</sub> in the VQE algorithm.

To investigate the degree of improvement in using a more accurate second-quantized Hamiltonian in a quantum VQE simulation that uses a heuristic hardware-

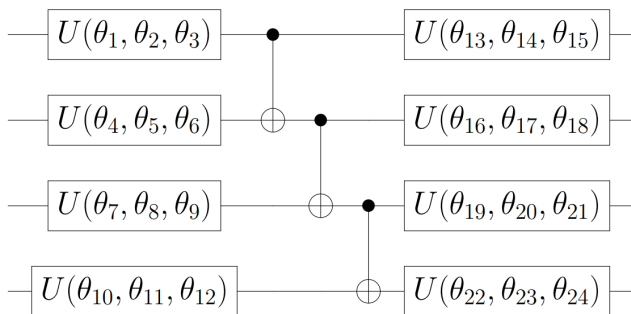


Figure 4. Four-qubit heuristic circuit ansatz for LiH in the VQE algorithm.

efficient wave-function preparation circuit [8, 58], we perform quantum simulation using the second-quantized Hamiltonians parameterized based on the minimal basis Daubechies wavelet molecular orbitals for  $H_2$  and LiH. We intend to compare our results with previous studies using a hardware-efficient VQE approach based on STO-3G Hamiltonian [8, 59], thus we remove the 2py and 2pz orbitals of LiH to use the same number of four qubits for the LiH system. In addition, our numerical experiment uses low-depth heuristic circuit *ansatzes* for hydrogen  $H_2$  (Fig. 3) and lithium hydride LiH molecule (Fig. 4), respectively, in the VQE algorithm. More importantly, instead of running on a noise-free simulator, we investigate the performance of the quantum simulations under noisy quantum-computer configurations to provide a more realistic simulation of a NISQ device. The noise model was obtained from a realistic error statistics of the “ibmq-santiago” device (see Appendix A for details), thus the simulations provide a realistic benchmark of quantum computations on near-term quantum hardware. Each energy point is the average of  $10^4$  shots in each iteration with readout-error mitigation.

Figure 5 shows the potential energy curves of the VQE simulations for  $H_2$  and LiH using a Hamiltonian represented by the minimal basis Daubechies wavelet molecular orbitals. For comparison, the results from the STO-3G basis set and respective classical FCI (labeled exact) calculations are also presented. The  $H_2$  energy curve obtained with the Daubechies wavelet Hamiltonian agrees well with the exact FCI results even in the noisy simulations (Fig. 5(a)), which we attribute to the small size of the system and the low circuit depth required for the VQE simulation.

The raw potential energy curve for LiH obtained with the Daubechies wavelet Hamiltonian is presented in Fig. 5(b), and it clearly deviates from the exact FCI result, indicating the stronger influence of noise in this larger calculation. Therefore, for LiH we also calculate the results in higher noise levels and correct the obtained energy by considering the linear zero-noise extrapolation method [60–62] for error mitigation. The mitigated energy curve then is in excellent agreement with the exact FCI result. Note that the UCCSD *ansatz* for minimal

basis LiH calculation requires about over 1000 quantum gates for state preparation, whereas the heuristic *ansatz* requires only about 11 quantum gates (Fig. 4). Our results strongly support the effectiveness of the low-depth heuristic *ansatz* when compared to the UCCSD *ansatz* (Fig. 1).

It is also worth noting that the minimal basis STO-3G and Daubechies wavelet molecular orbital potential energy curves are significantly different. While the state preparation using the low-depth heuristic *ansatz*, the Daubechies wavelet method yields results that are in excellent agreement with experimental data (Table I); in contrast, the STO-3G Hamiltonian yields poor results, and this cannot be improved by additional quantum resources. Our results emphasize the importance of using a high-quality Hamiltonian in heuristic VQE quantum simulations.

To quantify the computational errors, the deviations from their respective classical exact FCI curves for  $H_2$  and LiH are plotted in Figs. 5(c) and 5(d), respectively. In Fig. 5(c), we can see that most of the raw data achieve chemical accuracy for the hydrogen molecule by using the Daubechies wavelet basis set. Additionally, for LiH molecule (Fig. 5(d)), calculations without error mitigation using Daubechies wavelet molecular orbitals exhibit approximately 4 kcal/mol error, smaller than that of the STO-3G Hamiltonian. Compared to previously published calculations [8, 59], our simulation results demonstrate that the low-depth *ansatz* can be applied to obtain more accurate raw data by using the Daubechies wavelet basis. Furthermore, after applying the zero-noise extrapolation, most of the mitigated data achieve the chemical accuracy level. Note that the errors presented for the Daubechies wavelet and the STO-3G methods are obtained by comparing to their respective classical FCI calculations. If comparison with experimental data is concerned, the STO-3G data will exhibit a significant error, as discussed earlier. By using the minimal basis Daubechies wavelet molecular orbitals to present the Hamiltonian, it is demonstrated that more accurate results using the same quantum resources as STO-3G is possible. Therefore, the minimal basis Daubechies wavelet molecular orbitals provide significantly improved Hamiltonian representation, and thus is especially adapted to quantum simulation of molecular systems in this NISQ quantum era.

#### IV. CONCLUSION

In this work, we demonstrate that self-consistent field calculations based on a Daubechies wavelet basis set can prepare a better set of molecular orbitals, which in turn results in a better many-body Hamiltonian. The completeness and orthogonality, in both real and momentum space, allow Daubechies wavelet basis sets to produce accurate and efficient representations of molecular electronic systems. We show that quantum simulation

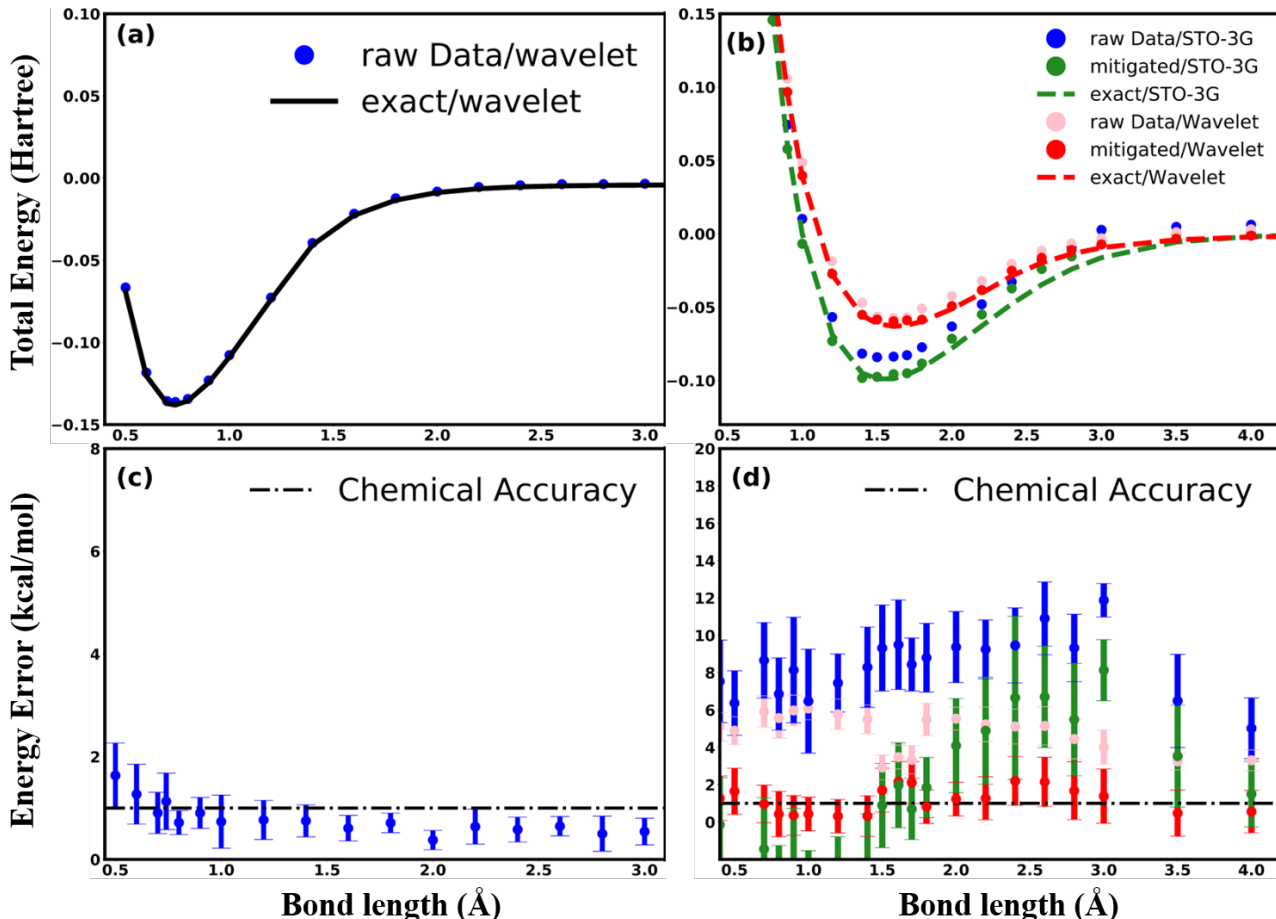


Figure 5. Potential energy curves and computational errors of  $\text{H}_2$  and  $\text{LiH}$  obtained from calculations under noisy environments. The errors presented for the Daubechies wavelet and the STO-3G methods are deviations from their respective classical exact FCI calculation values. (a)  $\text{H}_2$ . Results calculated using the minimal basis Daubechies wavelet molecular orbitals (blue dots) as well as the classical FCI (solid line) are shown. (b)  $\text{LiH}$ . The blue (pink) dots depict the raw data calculated from the STO-3G (DW) basis set. The green (red) dots denote the extrapolated energies over three different CNOT gate counts from the STO-3G (DW) basis set. These simulations with noise are averaged over ten sets of VQE experiments with  $10^4$  shots for each iteration. The solid lines are the respective classical FCI results. (c)  $\text{H}_2$  errors. The color scheme is the same as in the legend of (a). (d)  $\text{LiH}$  errors. The color scheme is the same as in the legend of (b). The error bars represent the 95% confidence uncertainties that take the standard error of experiments at each CNOT gate count and the residues of linear regression into account. Most of the errors after mitigation are within the chemical accuracy defined as 1 kcal/mol.

using the DW/UCCSD VQE method predicts accurate structures of small molecules ( $\text{H}_2$ ,  $\text{LiH}$ , and  $\text{H}_2\text{O}$ ) at a computational cost equivalent to the calculations using a minimal basis STO-3G basis set. The improved Daubechies wavelet molecular orbitals enable us to determine  $\text{H}_2$  and  $\text{LiH}$  vibrational frequencies with the values in excellent agreement with experimental data. Furthermore, we show that using a Hamiltonian represented in minimal basis Daubechies wavelet molecular orbitals together with a low-depth heuristic VQE state-preparation circuit yield excellent results with much fewer quantum gates compared to UCCSD ansatz. Our work indicates the importance of the choice of basis set in applying quantum computing to computational chemistry, and the Daubechies wavelet basis set is shown to be highly ad-

vantageous in terms of both accuracy and efficiency.

Introducing the Daubechies wavelet basis improves the quality of the Hamiltonian while keeping the quantum resources needed to implement it minimal. Furthermore, as the Daubechies wavelet molecular orbitals are constructed from a grid of wavelet functions, it bridges the grid method and the atomic orbital basis method for quantum computation of quantum chemistry. As a result, the Daubechies wavelet method proposed here yields results that are comparable to classical high-level basis set methods with predictive power for experimental observables. Note that the Daubechies wavelet basis offers means to systematically improve the accuracy of the calculations both in terms of the fineness of the Daubechies wavelet grids used to construct the molecular orbitals

and the number of virtual orbitals used in the post-HF calculations. Thus, conventional approaches to reduce the size of the active space as well as hybrid postprocessing approaches to mitigate errors in quantum computers are readily applicable to the Daubechies wavelet basis method [3, 26].

## V. ACKNOWLEDGMENTS

C.L.H is supported by the Young Scholar Fellowship (Einstein Program) of the Ministry of Science and Technology, Taiwan (R.O.C.) under Grants No. MOST 109-2636-E-002-001, No. MOST 110-2636-E-002-009, No. MOST 111-2119-M-007-006, and No. MOST 111-2119-M-001-004, by the Yushan Young Scholar Program of the Ministry of Education, Taiwan (R.O.C.) under Grants No. NTU-109V0904 and No. NTU-110V0904, and by the research project ‘‘Pioneering Research in Forefront Quantum Computing, Learning and Engineering’’ of National Taiwan University under Grant No. NTU-CC-111L894605. A.H. acknowledges funding support from City University of Hong Kong under Project No. 7005615, Hong Kong Institute for Advanced Study, City University of Hong Kong, under Project No. 9360157, and Research Grants Council of the Hong Kong Special Administrative Region, China under Project No. CityU 11200120. Y.C.C thanks the Ministry of Science and Technology, Taiwan (Grants No. MOST 109-2113-M-002-004 and No. MOST 109-2113-M-001-040), and National Taiwan University (Grant No. 110L890105) for financial support. H.S.G. acknowledges support from the the Ministry of Science and Technology, Taiwan under Grants No. MOST 109-2112-M-002-023-MY3, No. MOST 109-2627-M-002-003, No. MOST 107-2627-E-002-001-MY3, No. MOST 111-2119-M-002-006-MY3, No. MOST 109-2627-M-002-002, No. MOST 110-2627-M-002-003, No. MOST 110-2627-M-002-002, No. MOST 111-2119-M-002-007, No. MOST 109-2622-8-002-003, and No. MOST 110-2622-8-002-014, from the US Air Force Office of Scientific Research under Award Number FA2386-20-1-4033, and from the National Taiwan University under Grants No. NTU-CC-110L890102 and No. NTU-CC-111L894604. J.P.C., Y.C.C. and H.S.G. acknowledge support from the Physics Division, National Center for Theoretical Sciences, Taiwan.

### Appendix A: NOISY QUANTUM SIMULATION

We perform the numerical simulation using the IBM Qiskit simulator with the noise data downloaded from

the IBM Quantum 5-qubit machine `ibmq-santiago` on 16 May 2021. The qubit relaxation time  $T_1$ , dephasing time  $T_2$ , and qubit frequency data are listed in Table IV, the single-qubit gate error, gate length and readout error data are in Table V, and the two-qubit coupling and corresponding CNOT gate error and gate length data are listed in Table VI. Note that the IBM Quantum system service is still under active development, meaning that the noise data will change gradually

Table IV. Qubit relaxation time  $T_1$ , dephasing time  $T_2$  and qubit frequency data of the 5-qubit machine `ibmq-santiago` downloaded from the IBM Quantum system service at the time when the numerical simulation is performed

Qubit	$T_1$ ( $\mu$ s)	$T_2$ ( $\mu$ s)	Freq (GHz)
0	168.167	163.925	4.8334
1	145.087	96.712	4.6236
2	131.625	109.047	4.8205
3	175.273	85.200	4.7423
4	87.847	142.421	4.8163

Table V. Single-qubit gate errors, and readout error data of the 5-qubit machine `ibmq-santiago` downloaded from the IBM Quantum system service at the time when the experiment is performed.

Qubit	Gate error	Readout error
0	0.0264%	2.06%
1	0.0253%	1.29%
2	0.0194%	0.98%
3	0.0182%	0.62%
4	0.0232%	1.77%

Table VI. Two-qubit CNOT gate error and gate length data of the 5-qubit machine `ibmq-santiago` downloaded from the IBM Quantum system service at the time when the numerical simulation is performed. The two-qubit CNOT gate error and lengths are usually different for different two-qubit coupling pairs due to different coupling strength and different qubit frequencies in the qubit pairs

Coupling pair	Gate error	Gate length(ns)
[0, 1]	0.812%	526.22
[1, 0]	0.812%	561.78
[1, 2]	0.680%	355.55
[2, 1]	0.680%	320.00
[2, 3]	0.542%	376.89
[3, 2]	0.542%	412.44
[3, 4]	0.599%	376.89
[4, 3]	0.599%	341.33

[1] I. Kassal, J. D. Whitfield, A. Perdomo-Ortiz, M.-H. Yung, and A. Aspuru-Guzik, Simulating Chemistry Us-

ing Quantum Computers, *Annu. Rev. Phys. Chem.* **62**,

- 185 (2011).
- [2] Y. Cao, J. Romero, J. P. Olson, M. Degroote, P. D. Johnson, M. Kieferová, I. D. Kivlichan, T. Menke, B. Peropadre, N. P. D. Sawaya, S. Sim, L. Veis, and A. Aspuru-Guzik, Quantum Chemistry in the Age of Quantum Computing, *Chem. Rev.* **119**, 10856 (2019).
  - [3] S. McArdle, S. Endo, A. Aspuru-Guzik, S. C. Benjamin, and X. Yuan, Quantum computational chemistry, *Rev. Mod. Phys.* **92**, 015003 (2020).
  - [4] B. Bauer, S. Bravyi, M. Motta, and G. K.-L. Chan, Quantum Algorithms for Quantum Chemistry and Quantum Materials Science, *Chem. Rev.* **120**, 12685 (2020).
  - [5] A. Aspuru-Guzik, Simulated Quantum Computation of Molecular Energies, *Science* **309**, 1704 (2005).
  - [6] J. Du, N. Xu, X. Peng, P. Wang, S. Wu, and D. Lu, NMR Implementation of a Molecular Hydrogen Quantum Simulation with Adiabatic State Preparation, *Phys. Rev. Lett.* **104**, 030502 (2010).
  - [7] Y. Wang, F. Dolde, J. Biamonte, R. Babbush, V. Bergholm, S. Yang, I. Jakobi, P. Neumann, A. Aspuru-Guzik, J. D. Whitfield, and J. Wrachtrup, Quantum Simulation of Helium Hydride Cation in a Solid-State Spin Register, *ACS Nano* **9**, 7769 (2015).
  - [8] A. Kandala, A. Mezzacapo, K. Temme, M. Takita, M. Brink, J. M. Chow, and J. M. Gambetta, Hardware-efficient variational quantum eigensolver for small molecules and quantum magnets, *Nature* **549**, 242 (2017).
  - [9] J. I. Colless, V. V. Ramasesh, D. Dahlen, M. S. Blok, M. E. Kimchi-Schwartz, J. R. McClean, J. Carter, W. A. de Jong, and I. Siddiqi, Computation of Molecular Spectra on a Quantum Processor with an Error-Resilient Algorithm, *Phys. Rev. X* **8**, 011021 (2018).
  - [10] H. R. Grimsley, S. E. Economou, E. Barnes, and N. J. Mayhall, An adaptive variational algorithm for exact molecular simulations on a quantum computer, *Nat. Commun.* **10**, 3007 (2019).
  - [11] T. Bian, D. Murphy, R. Xia, A. Daskin, and S. Kais, Quantum computing methods for electronic states of the water molecule, *Mol. Phys.* **117**, 2069 (2019).
  - [12] Y. Nam, J.-S. Chen, N. C. Pisenti, K. Wright, C. Delaney, D. Maslov, K. R. Brown, S. Allen, J. M. Amini, J. Apisdorf, K. M. Beck, A. Blinov, V. Chaplin, M. Chmielewski, C. Collins, S. Debnath, K. M. Hudek, A. M. Ducore, M. Keesan, S. M. Kreikemeier, J. Mizrahi, P. Solomon, M. Williams, J. D. Wong-Campos, D. Moehring, C. Monroe, and J. Kim, Ground-state energy estimation of the water molecule on a trapped-ion quantum computer, *npj Quantum Inf.* **6**, 33 (2020).
  - [13] J. Preskill, Quantum Computing in the NISQ era and beyond, *Quantum* **2**, 79 (2018).
  - [14] M. A. Nielsen and I. L. Chuang, *Quantum computation and quantum information*, 10th ed. (Cambridge University Press, Cambridge ; New York, 2010).
  - [15] J. R. McClean, R. Babbush, P. J. Love, and A. Aspuru-Guzik, Exploiting Locality in Quantum Computation for Quantum Chemistry, *J. Phys. Chem. Lett.* **5**, 4368 (2014).
  - [16] R. Babbush, C. Gidney, D. W. Berry, N. Wiebe, J. McClean, A. Paler, A. Fowler, and H. Neven, Encoding Electronic Spectra in Quantum Circuits with Linear T Complexity, *Phys. Rev. X* **8**, 041015 (2018).
  - [17] D. W. Berry, M. Kieferová, A. Scherer, Y. R. Sanders, G. H. Low, N. Wiebe, C. Gidney, and R. Babbush, Improved techniques for preparing eigenstates of fermionic Hamiltonians, *npj Quantum Inf.* **4**, 22 (2018).
  - [18] A. Peruzzo, J. McClean, P. Shadbolt, M.-H. Yung, X.-Q. Zhou, P. J. Love, A. Aspuru-Guzik, and J. L. O’Brien, A variational eigenvalue solver on a photonic quantum processor, *Nat. Commun.* **5**, 4213 (2014).
  - [19] D. Wecker, M. B. Hastings, and M. Troyer, Progress towards practical quantum variational algorithms, *Phys. Rev. A* **92**, 042303 (2015).
  - [20] P. J. J. O’Malley, R. Babbush, I. D. Kivlichan, J. Romero, J. R. McClean, R. Barends, J. Kelly, P. Roushan, A. Tranter, N. Ding, B. Campbell, Y. Chen, Z. Chen, B. Chiaro, A. Dunsworth, A. G. Fowler, E. Jeffrey, E. Lucero, A. Megrant, J. Y. Mutus, M. Neeley, C. Neill, C. Quintana, D. Sank, A. Vainsencher, J. Wenner, T. C. White, P. V. Coveney, P. J. Love, H. Neven, A. Aspuru-Guzik, and J. M. Martinis, Scalable Quantum Simulation of Molecular Energies, *Phys. Rev. X* **6**, 031007 (2016).
  - [21] J. R. McClean, J. Romero, R. Babbush, and A. Aspuru-Guzik, The theory of variational hybrid quantum-classical algorithms, *New J. Phys.* **18**, 023023 (2016).
  - [22] W. J. Hehre, R. F. Stewart, and J. A. Pople, Self-Consistent Molecular-Orbital Methods. I. Use of Gaussian Expansions of Slater-Type Atomic Orbitals, *J. Chem. Phys.* **51**, 2657 (1969).
  - [23] Google AI Quantum and Collaborators, Hartree-Fock on a superconducting qubit quantum computer, *Science* **369**, 1084 (2020).
  - [24] R. Ditchfield, D. P. Miller, and J. A. Pople, Self-Consistent Molecular Orbital Methods. XI. Molecular Orbital Theory of NMR Chemical Shifts, *J. Chem. Phys.* **54**, 4186 (1971).
  - [25] T. H. Dunning, Gaussian basis sets for use in correlated molecular calculations. I. The atoms boron through neon and hydrogen, *J. Chem. Phys.* **90**, 1007 (1989).
  - [26] T. Takeshita, N. C. Rubin, Z. Jiang, E. Lee, R. Babbush, and J. R. McClean, Increasing the Representation Accuracy of Quantum Simulations of Chemistry without Extra Quantum Resources, *Phys. Rev. X* **10**, 011004 (2020).
  - [27] J. S. Kottmann, P. Schleich, T. Tamayo-Mendoza, and A. Aspuru-Guzik, Reducing Qubit Requirements while Maintaining Numerical Precision for the Variational Quantum Eigensolver: A Basis-Set-Free Approach, *J. Phys. Chem. Lett.* **12**, 663 (2021).
  - [28] P. Schleich, J. S. Kottmann, and A. Aspuru-Guzik, (2021), [ArXiv:2110.06812](https://arxiv.org/abs/2110.06812).
  - [29] I. Daubechies, *Ten lectures on wavelets* (Society for Industrial and Applied Mathematics, Philadelphia, Pa, 1992).
  - [30] A preliminary result of this work was presented as an invited talk of “Wavelet basis set meets quantum computing” delivered by the co-author, Jyh-Pin Chou, on Dec. 4, 2019 at the International Workshop on Quantum Computing, Information Processing and Machine Learning, Taipei, Taiwan. <https://webpageprodvm.ntu.edu.tw/CQSE2019workshop/>.
  - [31] S. Mohr, L. E. Ratcliff, L. Genovese, D. Caliste, P. Boulanger, S. Goedecker, and T. Deutsch, Accurate and efficient linear scaling DFT calculations with universal applicability, *Phys. Chem. Chem. Phys.* **17**, 31360 (2015).

- [32] L. E. Ratcliff, W. Dawson, G. Fisicaro, D. Caliste, S. Mohr, A. Degomme, B. Videau, V. Cristiglio, M. Stella, M. D’Alessandro, S. Goedecker, T. Nakajima, T. Deutsch, and L. Genovese, Flexibilities of wavelets as a computational basis set for large-scale electronic structure calculations, *J. Chem. Phys.* **152**, 194110 (2020).
- [33] L. Genovese, A. Neelov, S. Goedecker, T. Deutsch, S. A. Ghasemi, A. Willand, D. Caliste, O. Zilberberg, M. Rayson, A. Bergman, and R. Schneider, Daubechies wavelets as a basis set for density functional pseudopotential calculations, *J. Chem. Phys.* **129**, 014109 (2008).
- [34] S. Mohr, L. E. Ratcliff, P. Boulanger, L. Genovese, D. Caliste, T. Deutsch, and S. Goedecker, Daubechies wavelets for linear scaling density functional theory, *J. Chem. Phys.* **140**, 204110 (2014).
- [35] L. Genovese, B. Videau, M. Ospici, T. Deutsch, S. Goedecker, and J.-F. Méhaut, Daubechies wavelets for high performance electronic structure calculations: The BigDFT project, *Comptes Rendus Mécanique* **339**, 149 (2011).
- [36] R. Babbush, N. Wiebe, J. McClean, J. McClain, H. Neven, and G. K.-L. Chan, Low-Depth Quantum Simulation of Materials, *Phys. Rev. X* **8**, 011044 (2018).
- [37] I. D. Kivlichan, J. McClean, N. Wiebe, C. Gidney, A. Aspuru-Guzik, G. K.-L. Chan, and R. Babbush, Quantum Simulation of Electronic Structure with Linear Depth and Connectivity, *Phys. Rev. Lett.* **120**, 110501 (2018).
- [38] S. Goedecker, M. Teter, and J. Hutter, Separable dual-space Gaussian pseudopotentials, *Phys. Rev. B* **54**, 1703 (1996).
- [39] C. Hartwigsen, S. Goedecker, and J. Hutter, Relativistic separable dual-space Gaussian pseudopotentials from H to Rn, *Phys. Rev. B* **58**, 3641 (1998).
- [40] L. Genovese, T. Deutsch, A. Neelov, S. Goedecker, and G. Beylkin, Efficient solution of Poisson’s equation with free boundary conditions, *J. Chem. Phys.* **125**, 074105 (2006).
- [41] L. Genovese, T. Deutsch, and S. Goedecker, Efficient and accurate three-dimensional Poisson solver for surface problems, *J. Chem. Phys.* **127**, 054704 (2007).
- [42] S. B. Bravyi and A. Y. Kitaev, Fermionic Quantum Computation, *Ann. Phys. (N. Y)* **298**, 210 (2002).
- [43] J. T. Seeley, M. J. Richard, and P. J. Love, The Bravyi-Kitaev transformation for quantum computation of electronic structure, *J. Chem. Phys.* **137**, 224109 (2012).
- [44] S. Bravyi, J. M. Gambetta, A. Mezzacapo, and K. Temme, (2017), [ArXiv:1701.08213](https://arxiv.org/abs/1701.08213).
- [45] R. H. Byrd, P. Lu, J. Nocedal, and C. Zhu, A Limited Memory Algorithm for Bound Constrained Optimization, *SIAM J. Sci. Comput.* **16**, 1190 (1995).
- [46] J. Romero, R. Babbush, J. R. McClean, C. Hempel, P. J. Love, and A. Aspuru-Guzik, Strategies for quantum computing molecular energies using the unitary coupled cluster ansatz, *Quantum Sci. Technol.* **4**, 014008 (2018).
- [47] M.-H. Yung, J. Casanova, A. Mezzacapo, J. McClean, L. Lamata, A. Aspuru-Guzik, and E. Solano, From transistor to trapped-ion computers for quantum chemistry, *Sci. Rep.* **4**, 3589 (2015).
- [48] H. F. Trotter, On the product of semi-groups of operators, *Proc. Amer. Math. Soc.* **10**, 545 (1959).
- [49] A. Tranter, P. J. Love, F. Mintert, and P. V. Coveney, A Comparison of the Bravyi–Kitaev and Jordan–Wigner Transformations for the Quantum Simulation of Quantum Chemistry, *J. Chem. Theory Comput.* **14**, 5617 (2018).
- [50] H. R. Grimsley, D. Claudino, S. E. Economou, E. Barnes, and N. J. Mayhall, Is the Trotterized UCCSD Ansatz Chemically Well-Defined?, *J. Chem. Theory Comput.* **16**, 1 (2020).
- [51] P. K. Barkoutsos, J. F. Gonthier, I. Sokolov, N. Moll, G. Salis, A. Fuhrer, M. Ganzhorn, D. J. Egger, M. Troyer, A. Mezzacapo, S. Filipp, and I. Tavernelli, Quantum algorithms for electronic structure calculations: Particle-hole Hamiltonian and optimized wave-function expansions, *Phys. Rev. A* **98**, 022322 (2018).
- [52] M. S. ANIS, H. Abraham, AduOffei, R. Agarwal, G. Agliardi, M. Aharoni, I. Y. Akhalwaya, G. Aleksandrowicz, T. Alexander, M. Amy, S. Anagolum, E. Arbel, A. Asfaw, A. Athalye, A. Avkhadiev, C. Azaustre, A. Banerjee, S. Banerjee, W. Bang, A. Bansal, P. Barkoutsos, A. Barnawal, G. Barron, G. S. Barron, L. Bello, Y. Ben-Haim, D. Bevenius, D. Bhatnagar, A. Bhohe, P. Bianchini, L. S. Bishop, C. Blank, S. Bolos, S. Bopardikar, S. Bosch, S. Brandhofer, Brandon, S. Bravyi, N. Bronn, Bryce-Fuller, D. Bucher, A. Burov, F. Cabrera, P. Calpin, L. Capelluto, J. Carballo, G. Carrascal, I. Carvalho, A. Chen, C.-F. Chen, E. Chen, J. C. Chen, R. Chen, F. Chevallier, R. Cholarajan, J. M. Chow, *et al.*, [Qiskit: An Open-source Framework for Quantum Computing](https://arxiv.org/abs/2106.02661) (2021).
- [53] J. M. Turney, A. C. Simmonett, R. M. Parrish, E. G. Hohenstein, F. A. Evangelista, J. T. Fermann, B. J. Mintz, L. A. Burns, J. J. Wilke, M. L. Abrams, N. J. Russ, M. L. Leininger, C. L. Janssen, E. T. Seidl, W. D. Allen, H. F. Schaefer, R. A. King, E. F. Valeev, C. D. Sherrill, and T. D. Crawford, Psi4: an open-source *ab initio* electronic structure program: Psi4: an electronic structure program, *WIREs Comput. Mol. Sci.* **2**, 556 (2012).
- [54] R. M. Parrish, L. A. Burns, D. G. A. Smith, A. C. Simmonett, A. E. DePrince, E. G. Hohenstein, U. Bozkaya, A. Y. Sokolov, R. Di Remigio, R. M. Richard, J. F. Gonthier, A. M. James, H. R. McAlexander, A. Kumar, M. Saitow, X. Wang, B. P. Pritchard, P. Verma, H. F. Schaefer, K. Patkowski, R. A. King, E. F. Valeev, F. A. Evangelista, J. M. Turney, T. D. Crawford, and C. D. Sherrill, Psi4 1.1: An open-source electronic structure program emphasizing automation, advanced libraries, and interoperability, *J. Chem. Theory Comput.* **13**, 3185 (2017).
- [55] D. G. A. Smith, L. A. Burns, A. C. Simmonett, R. M. Parrish, M. C. Schieber, R. Galvelis, P. Kraus, H. Kruse, R. Di Remigio, A. Alenaizan, A. M. James, S. Lehtola, J. P. Misiewicz, M. Scheurer, R. A. Shaw, J. B. Schriber, Y. Xie, Z. L. Glick, D. A. Sirianni, J. S. O’Brien, J. M. Waldrop, A. Kumar, E. G. Hohenstein, B. P. Pritchard, B. R. Brooks, H. F. Schaefer, A. Y. Sokolov, K. Patkowski, A. E. DePrince, U. Bozkaya, R. A. King, F. A. Evangelista, J. M. Turney, T. D. Crawford, and C. D. Sherrill, Psi4 1.4: Open-source software for high-throughput quantum chemistry, *J. Chem. Phys.* **152**, 184108 (2020).
- [56] *Lange’s Handbook of Chemistry, Seventeenth Edition.* (McGraw-Hill Professional., Place of publication not identified, 2017) oCLC: 1096693900.
- [57] J. Lee, W. J. Huggins, M. Head-Gordon, and K. B. Whaley, Generalized Unitary Coupled Cluster Wave functions for Quantum Computation, *J. Chem. Theory Comput.*

- [15](#), 311 (2019).
- [58] M. Benedetti, E. Lloyd, S. Sack, and M. Fiorentini, Parameterized quantum circuits as machine learning models, [Quantum Sci. Technol.](#) **4**, 043001 (2019).
- [59] A. Kandala, K. Temme, A. D. Córcoles, A. Mezzacapo, J. M. Chow, and J. M. Gambetta, Error mitigation extends the computational reach of a noisy quantum processor, [Nature](#) **567**, 491 (2019).
- [60] T. Giurgica-Tiron, Y. Hindy, R. LaRose, A. Mari, and W. J. Zeng, Digital zero noise extrapolation for quantum error mitigation, in [2020 IEEE International Conference on Quantum Computing and Engineering \(QCE\)](#) (IEEE, Denver, CO, USA, 2020) pp. 306–316.
- [61] R. LaRose, A. Mari, S. Kaiser, P. J. Karalekas, A. A. Alves, P. Czarnik, M. E. Mandouh, M. H. Gordon, Y. Hindy, A. Robertson, P. Thakre, N. Shammah, and W. J. Zeng, (2021), [ArXiv:2009.04417](#) .
- [62] Y. Shee, P.-K. Tsai, C.-L. Hong, H.-C. Cheng, and H.-S. Goan, Qubit-efficient encoding scheme for quantum simulations of electronic structure, [Phys. Rev. Research](#) **4**, 023154 (2022).